PROCEEDINGS OF SCIENCE

3D structure of jet-induced diffusion wake in high-energy heavy-ion collisions

Zhong Yang,[a,*] **Tan Luo,**[b] **Wei Chen,**[c] **Longgang Pang**[a] **and Xin-Nian Wang**[a,d]

[a] *Key Laboratory of Quark and Lepton Physics (MOE) & Institute of Particle Physics, Central China Normal University, Wuhan 430079, China*

[b] *Instituto Galego de Física de Altas Enerxías IGFAE, Universidade de Santiago de Compostela, E-15782 Galicia-Spain*

[c] *School of Science, Wuhan University of Science and Technology Wuhan 430065, China*

[d] *Nuclear Science Division MS 70R0319, Lawrence Berkeley National Laboratory, Berkeley, California 94720, USA*

E-mail: yangzhong1994@mails.ccnu.edu.cn, xnwang@lbl.gov

Diffusion wake that accompanies the jet-induced Mach cone provides a unique probe of the properties of quark-gluon plasma in high-energy heavy-ion collisions. It can lead to a depletion of soft hadrons in the opposite direction of the propagating jet. We explore the 3D structure of the diffusion wake induced by γ triggered jets in Pb+Pb collisions at the LHC energy within the coupled linear Boltzmann transport and hydro model. We find a valley structure caused by the diffusion wake on top of the initial multiple parton interaction (MPI) ridge in rapidity and azimuthal angle. This results in a double-peak structure in the rapidity distribution of soft hadrons in the opposite direction of the jets as an unambiguous signal of the diffusion wake. We use a two-Gaussian fitting method to extract the diffusion wake and MPI contributions to the double peak. The diffusion wake valley is found to deepen with the jet energy loss as characterized by the γ-jet asymmetry. Its sensitivity to medium properties such as the equation of state and shear viscosity is also studied.

HardProbes2023
26-31 March 2023
Aschaffenburg, Germany

*Speaker

PoS(HardProbes2023)124

1. Introduction: The strongly coupled quark gluon plasma(QGP) can be formed in high-energy heavy-ion collisions[1, 2]. Jets generated in the initial hard scattering will go through the QGP medium and interact with it. Such interaction will lead to jet-induced medium response in the form of Mach-cone-like excitation. Studying of jet-induced medium response can help us glean properties of QGP such as the bulk transport properties and the equation of state(EoS).

The diffusion wake, an integral component of jet-induced Mach cone, can lead to the depletion of soft hadrons in the final hadron spectra in the opposite direction of the propagating jet[3, 8–10]. It is an unambiguous signal of jet-induced medium response. However, this signal is challenging to observe in both theoretical and experimental results due to the overwhelming contribution from initial multiple parton interactions (MPI). To get this signal, we must perform a mixed-event MPI subtraction to isolate its contribution, or alternatively, use 2D jet tomography to select events with specific jet starting positions to amplify the signal of jet-induced diffusion wake[3].

Since the jet-induced Mach cone is a 3D object, the diffusion wake should also have an interesting 3D structure in an expanding QGP in heavy-ion collisions. To study its 3D structure, We will carry out the jet-hadron correlation in rapidity and azimuthal angle in γ-jet events in Pb+Pb collisions at LHC. We will show that a unique valley structure is formed in the opposite direction of the γ-triggered jet on top of a ridge from MPI due to the diffusion wake. Using a two-Gaussian fit,we can extract the MPI ridge and the diffusion wake valley. Then We will study the sensitivity of the diffusion wake valley to jet energy loss, EoS and shear viscosity.

2. The model setup: We use the CoLBT-hydro model to simulate γ-jet propagation and jet-induced medium response in Pb+Pb collisions at the LHC. CoLBT-hydro combines the linear Boltzmann transport (LBT) model[4, 5] with the event-by-event (3+1)D CCNU-LBNL viscous (CLVisc) hydrodynamic model[6]. The initial configurations of γ-jet are generated by the PYTHIA8. The initial transverse position of γ-jet and the initial energy density of CLVisc model are provided by the Trento model. The propagation of jet parton and recoil parton in QGP is simulated by the LBT model which is based on the Boltzmann equation. The CLVisc model is responsible for the evolution of the bulk medium and soft partons in the CoLBT-hydro model. A combination of a freeze-out temperature T_f=137 MeV and specific shear viscosity η/s=0.15, along with the s95p parameterization of lattice QCD EoS with a rapid crossover and the initial condition with a longitudinal envelope at an initial time τ_0=0.6fm/c, is employed in the CLVisc to reproduce experimental data on bulk hadron spectra and anisotropic flows at the LHC.

During each time step of the CoLBT-hydro simulation, we need to sort jet and recoil partons according to a cut-off parameter p^0_{cut}, which is set to 2 GeV in this work. If parton's energy in the local rest frame is greater than p^0_{cut}, it will be classified as a hard parton and can still be described by the LBT model. Conversely, if the energy is less than the cut-off parameter, it is considered to be a soft parton. The soft partons and negative partons from the backreaction in the LBT model will serve as source terms for the CLVisc model through Gaussian smearing.

$$J^\nu = \sum_i \frac{\theta(p^0_{cut} - p_i \cdot u)p^\nu}{\tau(2\pi)^{3/2}\sigma_r^2\sigma_{\eta_s}\Delta\tau} e^{-\frac{(\vec{x}_\perp - \vec{x}_{\perp i})^2}{2\sigma_r^2} - \frac{(\eta_s - \eta_{si})^2}{2\sigma_{\eta s}^2}} \tag{1}$$

where σ_r and σ_{η_s} are Gaussian widths in transverse and longitudianl direction, respectively. We take σ_r=σ_{η_s}=0.3 fm in this work.

The final hadron spectra of CoLBT-hydro model is contributed by two parts. One is the hadronization of hard partons within a parton recombination model, the other is the jet-induced hydro response via Cooper-Frye freeze-out after subtracting the background from the same hydro event without the γ-jet.

3. Results: We use the γ-jet with the following kinetic cuts to study the 3D structure of diffusion wake. $p_T^{\rm jet} > 30$GeV/c, $|\eta^{\rm jet}| < 1.6$, $p_T^{\gamma} > 60$GeV/c, $|\eta^{\gamma}| < 1.44$, $|\Delta\phi_{\gamma \rm jet}| > 7/8\pi$ and R=0.3. Firstly, we plot in Fig. 1 the jet-hadron correlations in $\Delta\eta = \eta_h - \eta_{\rm jet}$ and $\Delta\phi = \phi_h - \phi_{\rm jet}$ for soft hadrons in $p_{\rm T} \in (0, 2)$ GeV/c in (a) p+p and (b) 0-10% central Pb+Pb collisions at $\sqrt{s_{\rm NN}} = 5.02$ TeV. In p+p collisions, there is a peak along the jet direction, it is contributed by the hadrons from the jet and MPI. In Pb+Pb collisions, this peak is clearly enhanced due to jet-induced medium response and medium-induced gluon radiation. Meanwhile, in the opposite to the jet axis where $|\Delta\phi| > \pi/2$, a valley is formed on top of the MPI ridge due to the depletion of soft hadrons by jet-induced diffusion wake. Therefore, we refer this as the diffusion wake (DF-wake) valley. We think this valley in rapidity $\Delta\eta$ as a unique signal of the diffusion wake.

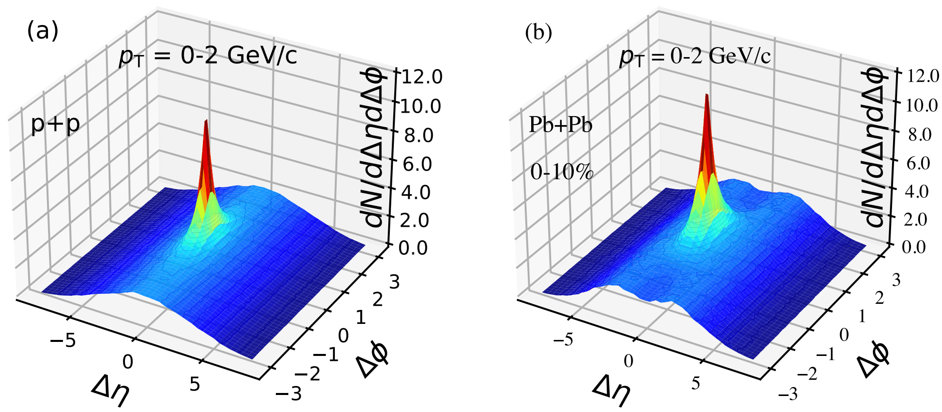

Figure 1: CoLBT-hydro results on γ-triggered jet-hadron correlation for soft hadrons ($p_{\rm T}$ = 0-2 GeV/c) in $\Delta\eta = \eta_h - \eta_{\rm jet}$ and $\Delta\phi = \phi_h - \phi_{\rm jet}$ in (a) p+p and (b) 0-10% Pb+Pb collisions at $\sqrt{s_{\rm NN}} = 5.02$ TeV.

To have a detailed understanding of this DF-wake valley, we plot in Fig. 2(a) the jet-hadron correlation as a function of rapidity $\Delta\eta$ in the region $|\Delta\phi| > \pi/2$. The purpose of doing this is to reduce the interference of jet partons on this valley. We also plot jet-hadron correlation as a function of $\Delta\phi$ in the region $|\Delta\eta| < 2.2$ in Fig. 2(b). In p+p collisions, the Gaussian-like MPI ridge in the rapidity distribution of the jet-hadron correlation comes from independent mini-jets in MPI. In Pb+Pb collisions, these mini-jets are also quenched, leading to an enhancement of soft hadrons and a suppression of high p_T hadrons. The DF-wake valley on top of the MPI ridge gives rise to a double peak feature in the rapidity distribution in Fig. 2(a) The deepest DF-wake valley occurs in the direction opposite to the jet axis ($|\Delta\phi| = \pi$). As one moves toward the jet-axis in azimuthal angle, the valley gradually gives away to the jet peak starting at around $|\Delta\phi| \leq \pi/2$ as seen in Figs. 1(b) and 2(b).

To further extract the diffusion wake and MPI contributions to the double peak in the rapidity

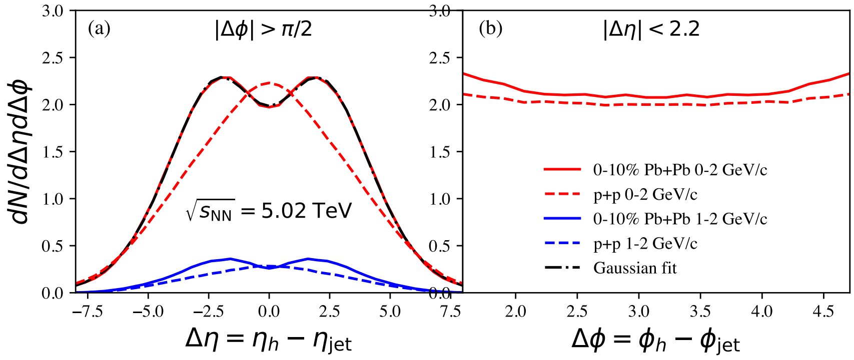

Figure 2: CoLBT-hydro results on γ-triggered jet-hadron correlation (a) in $\Delta\eta$ within $|\Delta\phi| > \pi/2$ and (b) in $\Delta\phi$ within $|\Delta\eta| < 2.2$ for soft hadrons within $p_{\rm T}$ = 0-2 GeV/c (red) and $p_{\rm T}$ = 1-2 GeV/c range (blue) in p+p (dashed) and 0-10% central Pb+Pb (solid) collisions at $\sqrt{s_{\rm NN}}$ = 5.02 TeV. The black dot-dashed line is the 2-Gaussian fit using Eq. (2).

distribution of jet-hadron correlation in Pb+Pb collisions, we employ the two-Gaussian

$$F(\Delta\eta) = \int_{\eta_{j1}}^{\eta_{j2}} d\eta_j F_3(\eta_j)(F_2(\Delta\eta,\eta_j) + F_1(\Delta\eta)), \tag{2}$$

to fit our result, where $F_1(\Delta\eta) = A_1 e^{-\Delta\eta^2/\sigma_1^2}$ is the Gaussian-like DF-wake valley, $F_2(\Delta\eta,\eta_j) = A_2 e^{-(\Delta\eta+\eta_j)^2/\sigma_2^2}$ is the Gaussian-like MPI ridge, $F_3(\eta_j)$ is the self-normalized Gaussian-like rapidity distribution of γ-triggered jets from CoLBT-hydro simulations, and $\eta_{j1,j2}$ define the jet rapidity range in the analysis. The dot-dashed line in Fig. 2(a) demonstrates the robustness of the 2-Gaussian fit to the double peak structure.

With the two-Gaussian fitting method, we first study the relationship between the DF-wake valley and jet energy loss. We use γ-jet asymmetry $x_{j\gamma}$ to select events with different jet energy loss. Shown in Fig. 3 are the rapidity distributions of (a) the DF-wake valley and (b) MPI ridge from the 2-Gaussian fit to the jet-hadron correlation in 0-10% central Pb+Pb collisions in $|\Delta\phi > |\pi/2$ for $x_{j\gamma} < 0.6$ (red solid), $x_{j\gamma} \in (0.6, 1.0)$ (blue dashed) and $x_{j\gamma} > 1$ (black dot-dashed). In Fig. 3, events with small $x_{j\gamma}$ usually have a deeper DF-wake valley, as jet propagation length is longer and energy loss is larger in these events. On the other hand, the MPI ridge has a very weak and non-monotonic dependence on $x_{j\gamma}$ due to the non-monotonic dependence of the propagation length on $x_{j\gamma}$ for minijets from MPI.

We also check the sensitivity of the diffusion wake to medium properties such as shear viscosity and EOS in this work. To study the sensitivity to the shear viscosity, we carry out CoLBT-hydro simulations of the same γ-jet events with two different values of η/s = 0.0 and 0.15 in CLVisc. Fig. 4 are the corresponding rapidity distributions of the DF-wake valley(a) and MPI ridge(b) in the opposite direction of the jet. We find that the DF-wake valley is slightly deeper and the MPI ridge is smaller in viscous hydro. Because shear viscosity will increase the transverse flow velocity as compared to the ideal hydro and thus increase the slope of hadron p_T spectra. This will suppress the MPI ridge and reduce the DF-wake valley of soft hadrons. Meanwhile, the negative shear correction of the longitudinal pressure in the energy-momentum tensor will impede the longitudinal

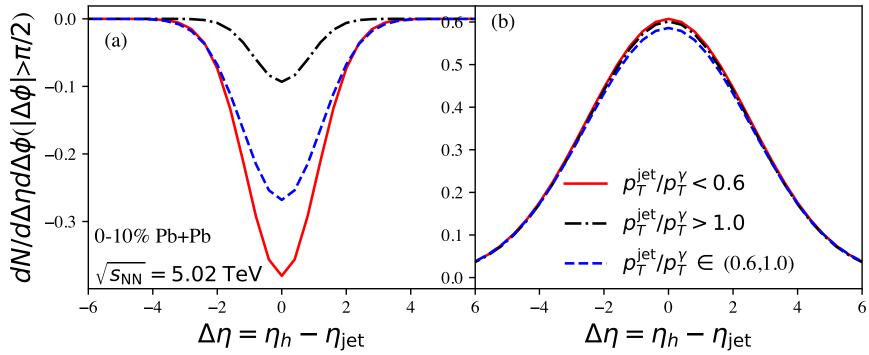

Figure 3: (a) Diffusion wake valley and (b) MPI ridge in γ-triggered jet-hadron correlation in $|\Delta\phi| > \pi/2$ as a function of $\Delta\eta$ with different ranges of $x_{j\gamma} = p_T^{jet}/p_T^{\gamma}$ in 0-10% central Pb+Pb collisions at $\sqrt{s_{NN}} = 5.02$ TeV from CoLBT-hydro.

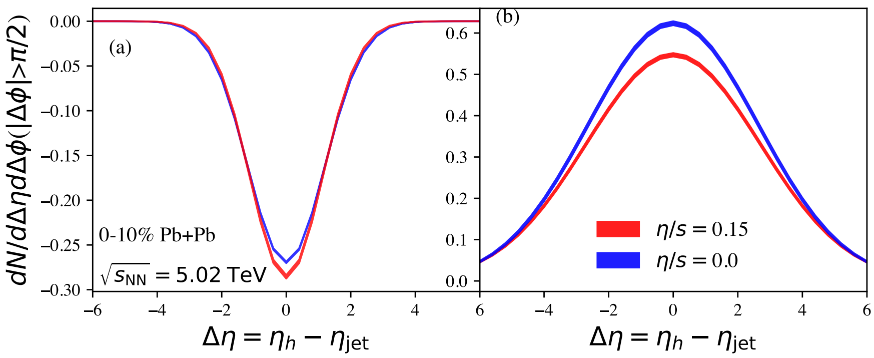

Figure 4: The same as Fig. 3 except with different values of specific shear viscosity η/s in CoLBT-hydro. Bands are numerical errors.

expansion. This will increase the MPI ridge and deepen the DF-wake valley in rapidity. These two effects competes and results in the distinction between viscous and ideal hydro in Fig. 4.

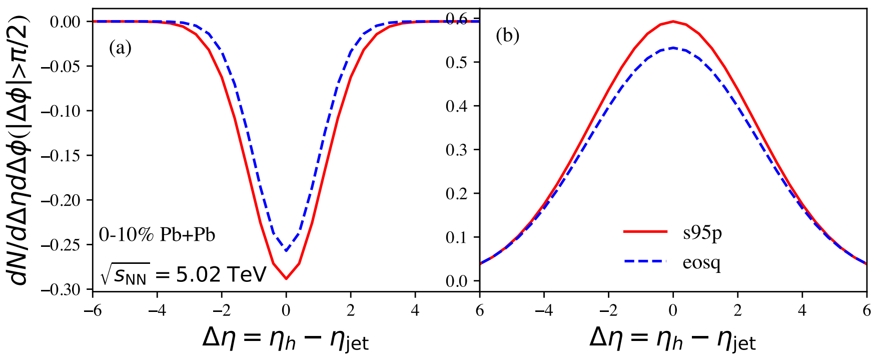

Figure 5: The same as Fig. 3 except with two different EoS: s95p (solid) and eosq (dashed) in CoLBT-hydro.

To check the sensitivity of the DF-wake valley to EoS, we consider an EoS (eosq) with a first-order phase transition instead of the default EoS (s95p-v1) with a rapid crossover in CLVisc.

PoS(HardProbes2023)124

According to the Fig. 5, we find the DF-wake valley is shallower and MPI ridge is smaller in the case of EoS eosq as compared to s95p. These differences are caused by the effective sound velocity which is higher in eosq than s95p EoS. Because a higher sound velocity leads to a larger Mach cone angle and the DF-wake spreads between the Mach cone behind the wave front, therefore a shallower DF-wake valley is formed. Meanwhile, a higher sound velocity will also result in a stronger radial flow, which reduces the soft hadron yield from MPI and the DF-wake valley similarly to increasing the shear viscosity.

Acknowledgement: This work is supported in part by NSFC under Grant Nos. 11935007, 11861131009, 11890714 and 12075098, by Fundamental Research Funds for Central Universities in China, by DOE under Contract No. DE-AC02-05CH11231, by NSF under Grant No. ACI-1550228 within the JETSCAPE and OAC-2004571 within the X-SCAPE Collaboration, by EU ERDF and H2020 grant 82409, ERC grant ERC-2018-ADG-835105, Spanish AEI grant FPA2017-83814-P and MDM- 2016-0692, Xunta de Galicia Research Center accreditation 2019-2022. Computations in this study are performed at the NSC3/CCNU and NERSC.

References

[1] K. Adcox *et al.* [PHENIX], Phys. Rev. Lett. **88**, 022301 (2002) doi:10.1103/PhysRevLett.88.022301 [arXiv:nucl-ex/0109003 [nucl-ex]].

[2] C. Adler *et al.* [STAR], Phys. Rev. Lett. **89**, 202301 (2002) doi:10.1103/PhysRevLett.89.202301 [arXiv:nucl-ex/0206011 [nucl-ex]].

[3] W. Chen, Z. Yang, Y. He, W. Ke, L. Pang and X. N. Wang, Phys. Rev. Lett. **127** (2021) no.8, 082301 doi:10.1103/PhysRevLett.127.082301 [arXiv:2101.05422 [hep-ph]].

[4] T. Luo, Y. He, S. Cao and X. N. Wang, [arXiv:2306.13742 [nucl-th]].

[5] Y. He, T. Luo, X. N. Wang and Y. Zhu, Phys. Rev. C **91**, 054908 (2015) [erratum: Phys. Rev. C **97**, no.1, 019902 (2018)] doi:10.1103/PhysRevC.91.054908 [arXiv:1503.03313 [nucl-th]].

[6] L. G. Pang, H. Petersen and X. N. Wang, Phys. Rev. C **97**, no.6, 064918 (2018) doi:10.1103/PhysRevC.97.064918 [arXiv:1802.04449 [nucl-th]].

[7] X. Y. Wu, G. Y. Qin, L. G. Pang and X. N. Wang, Phys. Rev. C **105**, no.3, 034909 (2022) doi:10.1103/PhysRevC.105.034909 [arXiv:2107.04949 [hep-ph]].

[8] W. Chen, S. Cao, T. Luo, L. G. Pang and X. N. Wang, Phys. Lett. B **777**, 86-90 (2018) doi:10.1016/j.physletb.2017.12.015 [arXiv:1704.03648 [nucl-th]].

[9] Z. Yang, T. Luo, W. Chen, L. G. Pang and X. N. Wang, Phys. Rev. Lett. **130**, no.5, 052301 (2023) doi:10.1103/PhysRevLett.130.052301 [arXiv:2203.03683 [hep-ph]].

[10] Z. Yang, Y. He, W. Chen, W. Y. Ke, L. G. Pang and X. N. Wang, [arXiv:2206.02393 [nucl-th]].